

MILITARY TECHNICAL COLLEGE
CAIRO - EGYPT



7th INTERNATIONAL CONF. ON
AEROSPACE SCIENCES &
AVIATION TECHNOLOGY

A DYNAMIC MODEL OF A SINGLE LINK FLEXIBLE MANIPULATOR

M. M. HEGAZE* , A. S. ABD EL-MOHSEN**

ABSTRACT

Motivated by the need to improve their productivity, interest has grown in the past few years in the study of flexible robot manipulators dynamics and control. In this work, a dynamic model of a Single link flexible manipulator based on the assumed mode method is presented. The manipulator has been considered as a Bernoulli-Euler beam subjected to finite rotation. A computer program including the proposed model has been used to simulate numerically the dynamic response of a manipulator under investigation. The validity of the proposed model has been verified through the comparison between the dynamic response of the manipulator based on the proposed model and that based on a Finite Element model.

The proposed model has been used to investigate the contribution of the main mechanical design parameters (damping, and payload) as well as the open loop control torque profile on the performance of the manipulator under investigation.

NOMENCLATURE

A	cross-section area of the link.	$[r_1^1]$	the position vector of the point in the undeformed configuration.
a_i	the modal coordinates.	T	Kinetic energy.
C_i	constants depends on the natural frequency	$[T_0^1]$	a homogenous transformation matrix
$[d_1]$	the elastic displacement vector .	V	Potential energy.
E	modules of elasticity	V_1	lateral displacement of a point on the neutral axis
$E I_z$	bending rigidity of the manipulator.	V_p	absolute velocity of the payload
g	gravitational acceleration.	V_{eL}	gravitational potential energy of the link
I_r	mass moment of inertia of the rotor.	V_{ep}	gravitational potential energy of the payload
I_z	area moment of inertia of the link.	Y_i	the modal shape functions.
L	length of the link	$\beta_i L$	the solution of the characteristic eqn.
m_p	mass of the payload	θ_F	the joint angle corresponding to the flexible manipulators
M	applied motor torque at the joint.	θ_R	the joint angle corresponding .to the rigid manipulators
q_i	i^{th} generalized coordinate.	ξ_i	i^{th} damping factor
Q_i	i^{th} generalized forces.	ρ	specific mass of the link material.
$[r_p]$	absolute velocity of the tip point	ω_i	i^{th} natural frequency.

* Assistant, Dpt. of Mechanics, M.T.C., Cairo, Egypt ** Professor, Dpt. of Aeronautics, M.T.C., Cairo, Egypt.

INTRODUCTION

The efficiency of a single link flexible manipulator moving at high speed and having a payload is highly dependent on its dynamic behavior. The Lagrangian Mechanics and the assumed mode method have been used to derive a proposed dynamic model of a single link flexible manipulator having a revolute joint. The link has been considered as an Euler-Bernoulli beam subjected to large angular displacement. The kinematics of a single link flexible manipulator are described, here, based on the Equivalent Rigid Link System and a transformation matrix method. The overall motion of the flexible link consists of the Rigid Body Motion which is defined by the joint angle, and the Elastic Motion which is defined by the first two modal coordinates. Hence, the Euler-Bernoulli beam is converted from continuous system to discrete system having three generalized coordinates. The validity of the proposed model has been verified through the comparison between the dynamic response of the manipulator based on the proposed model and that based on a Finite Element Model [1]. The proposed model has been used to investigate the effect of three main design parameters, the payload, the damping, and the open-loop control torque profile.

KINEMATICS OF A SINGLE LINK FLEXIBLE MANIPULATOR.

The kinematic properties of a single link flexible manipulator are based on the Equivalent Rigid Link System and the transformation matrix. The Equivalent Rigid Link System of a flexible manipulator describes the Rigid Body Motion of the manipulator. While, the Equivalent Rigid Link System (ERLS) is defined as a hypothetical system which produces the Rigid Body Motion and, the Elastic Motion arising from the structural flexibility may be superimposed on it. A single-link flexible manipulator is shown in Fig.(1). The motion of the link is limited to the vertical plane. The flexible link can be bend freely in the vertical plane, while, it is stiff in torsion and horizontal bending. The link is represented by a steel flat bar clamped to an electric motor. The axis of rotation of the motor is the z axis.

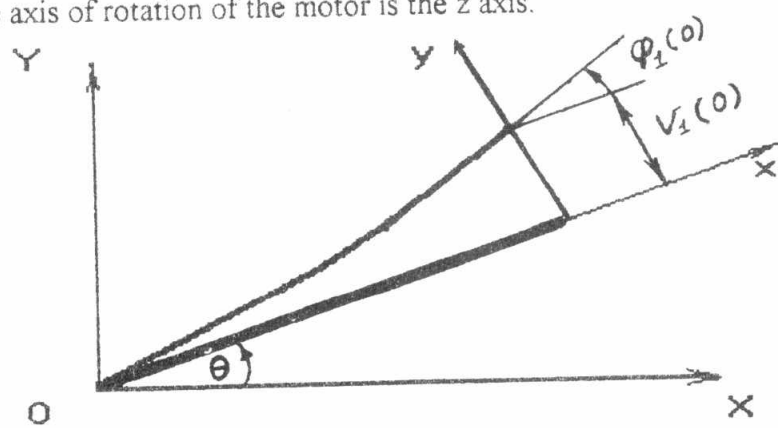


Fig.(1) Geometric and generalized coordinates of a flexible link.

For the case of a single link manipulator presented in Fig.(1), XY is the inertial frame. xy is a frame assigned to the Rigid Body. The position vector $[r_1]$ of an arbitrary point on the link with respect to the inertial frame can be expressed as,

$$[r_1] = [T_0^1] ([r_1^1] + [d_1])$$

A MATHEMATICAL MODEL OF A SINGLE LINK FLEXIBLE MANIPULATOR.

The model of the single link manipulator is obtained on the basis of Lagrange's equations of motion which may be written as .

$$\frac{d}{dt} \left(\frac{\partial T}{\partial \dot{q}_i} \right) - \frac{\partial T}{\partial q_i} + \frac{\partial V}{\partial q_i} = Q_i \quad i=1,2,\dots,n \quad (1)$$

The derivation of the manipulator mathematical model necessitates the determination of expression of its kinetic energy, potential energy, and generalized forces. These expressions are obtained here after

The assumed mode method is used to describe the lateral elastic displacement of the manipulator. Two modal shape functions are used to define the displacement field as follows .

$$V_1(x, t) = \sum_{i=1}^2 a_i(t) Y_i(x) \quad (2)$$

The natural modal functions corresponding to clamped-free uniform beam are used here [3, 4]. These modal functions are given by,

$$Y_i(x) = C_i (\cos \beta_i x + \cosh \beta_i x) + \sin \beta_i x + \sinh \beta_i x \quad (3)$$

$$C_1 = \frac{\sin \beta_1 L + \sinh \beta_1 L}{\cos \beta_1 L + \cosh \beta_1 L}$$

$$\beta_1 L = 1.875104069 \quad \beta_2 L = 4.694091133$$

$$\beta^4 = \frac{\omega^2 \rho A}{E I_z}$$

RELATION BETWEEN THE MODAL COORDINATES AND TIP POINT DISPLACEMENTS.

From eqn.(2) the elastic displacement is represented as a superposition of the first two modal coordinates as shown,

$$V_1(x,t) = a_1 Y_1 + a_2 Y_2$$

The slope angle is therefore given by,

$$\varphi_1(x, t) = \frac{\partial V_1(x, t)}{\partial x}$$

Hence, the tip point displacements are expressed as,

$$V_1(0) = 2a_1 C_1 + 2a_2 C_2 \quad (4)$$

$$\varphi_1(0) = 2a_1 \beta_1 + 2a_2 \beta_2 \quad (5)$$

GENERALIZED COORDINATES.

For a single-link flexible manipulator, the generalized coordinates are chosen to describe the overall motion of the flexible link. The overall motion of the link consists of the Rigid Body Motion which is defined by the joint angle θ , and the Elastic Motion which is defined by the first two modal coordinates a_1 and a_2 . The vector of generalized coordinates may therefore be given by,

$$\begin{bmatrix} q_1 \\ q_2 \\ q_3 \end{bmatrix} = \begin{bmatrix} \theta \\ a_1 \\ a_2 \end{bmatrix}$$

KINETIC ENERGY.

The total kinetic energy T of the manipulator system consists of three parts, the kinetic energy of the link T_L , the kinetic energy of the motor rotor T_r , and the kinetic energy of the payload T_p .

THE KINETIC ENERGY OF THE LINK T_L

The kinetic energy of the link is associated with the distributed mass along the length of the link, it is expressed as,

$$T_L = \frac{1}{2} \int_{\text{Link}} \left[\dot{r}_1 \right]^T \left[\dot{r}_1 \right] dm \quad (6)$$

THE KINETIC ENERGY OF THE ROTOR T_r

The kinetic energy associated with the rigid rotation of the rotor by an angular velocity $\dot{\theta}$ is expressed as,

$$T_r = \frac{1}{2} I_r \dot{\theta}^2 \quad (7)$$

THE KINETIC ENERGY OF THE PAYLOAD T_p

The kinetic energy of the payload is associated with the payload mass at $x = 0$, it is expressed as,

$$T_p = \frac{1}{2} \int_{\text{payload}} \left[\dot{r}_p \right]^T \left[\dot{r}_p \right] dm \quad (8)$$

The total kinetic energy T of the manipulator system is the sum of three terms T_L, T_r , and T_p ,

$$T = T_L + T_r + T_p$$

POTENTIAL ENERGY

The total potential energy V of the manipulator consists of, the strain energy V_s , and the gravitational potential energy V_g .

STRAIN ENERGY

The strain energy is due to the elastic deformation of the beam. For Bernauli-Euler beam the strain energy is given by;

$$V_s = \frac{1}{2} \int_{\text{link}} E I_x \left(\frac{\partial^2 V_1}{\partial X^2} \right)^2 dx$$

GRAVITATIONAL POTENTIAL ENERGY OF LINK

The gravitational potential energy of the link referred to the ZX plane as a datum is,

$$V_{gL} = \int_{\text{arm}} [\mathbf{r}_1]^T [\mathbf{g}] dm$$

GRAVITATIONAL POTENTIAL ENERGY OF PAYLOAD

Considering ZX plane as a datum, the gravitational potential energy of the payload is,

$$V_{gp} = m_p g (r_y)_{\text{at } x=0}$$

The total potential energy V may then be obtained as,

$$V = V_s + V_{gL} + V_{gp}$$

GENERALIZED FORCE.

It is assumed that the manipulator is applied upon only by a torque along the rotary joint axis, (motor torque). The generalized force is therefore given by,

$$[\mathbf{Q}] = [\mathbf{M} \ 0 \ 0]^T \tag{9}$$

EQUATIONS OF MOTION.

The application of Lagrange's eqn.(1) yields two sets of equations. The first set is associated with the Rigid Body degree of freedom defined by θ and the other set is associated with the Elastic degrees of freedom defined by a_1 and a_2 . These two sets of equations of motion for a single-link flexible manipulator are nonlinear time-varying coupled, second-order ordinary differential equations.

EQUATION OF MOTION ASSOCIATED WITH THE RIGID BODY MOTION.

Consider the generalized coordinate $q_1 = \theta$. Then, the equation of motion which describes the Rigid Body Motion is obtained as,

$$\frac{d}{dt} \left(\frac{\partial T}{\partial \dot{\theta}} \right) - \frac{\partial T}{\partial \theta} + \frac{\partial V}{\partial \theta} = Q_\theta \tag{10}$$

EQUATION OF MOTION ASSOCIATED WITH MODAL COORDINATES.

Consider the generalized coordinate $q_2 = a_1$. The substitution with the different terms into eqn.(1) yields, the equation of motion associated with a_1 as,

$$\frac{d}{dt} \left(\frac{\partial T}{\partial \dot{a}_1} \right) - \frac{\partial T}{\partial a_1} + \frac{\partial V}{\partial a_1} = Q_{a_1} \quad (11)$$

Consider the generalized coordinate $q_3 = a_2$. The substitution with the different terms into eqn.(1) yields, the equation of motion associated with a_2 as,

$$\frac{d}{dt} \left(\frac{\partial T}{\partial \dot{a}_2} \right) - \frac{\partial T}{\partial a_2} + \frac{\partial V}{\partial a_2} = Q_{a_2} \quad (12)$$

MODEL VALIDATION AND CASE STUDY.

This section is devoted to discussions concerning the validation of the model and the investigation of effect of its main design parameter on its performance.

VALIDATION OF THE PROPOSED DYNAMIC MODEL.

The validation of the proposed dynamic model is needed to ensure confidence of the model for use in the future design and control applications. To validate the dynamic model, the model simulation results corresponding to its dynamic response is compared with the dynamic response of a finite element model presented by Daniel [1]. The physical manipulator models for both cases have the same geometric, and mass properties, and are subjected to the same input torque profile as shown in Fig.(2).

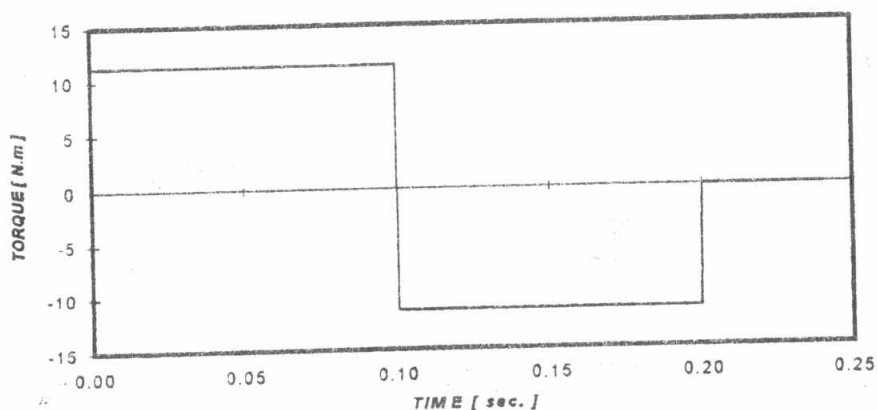


Fig.(2) Bang-bang open loop control torque profile

The numerical simulation of the proposed model is based on the numerical solution of Eqns.(10,11,12) using the Rung Kutta four method. A computer programs in FORTRAN have been prepared for this purpose. Fig.(3) shows the time history of the joint angle θ corresponding to the Finite Element model of the flexible manipulator (thin line) [1]. On the same figure in thick line is shown the time history of θ corresponding the rigid manipulator. Fig.(4) shows the time history of the joint angle θ corresponding to the flexible manipulator based on the proposed model (thin line).

On the same figure in thick line is shown the time history of θ corresponding the rigid manipulator. The comparison between Fig.(4) and Fig.(3) shows that for $0 \leq t \leq 0.2$ sec. there is a good agreement between the proposed manipulator model and the Finite Element model [1]. The sustained vibration observed for $t > 0.2$ sec. is justified by the lack of damping in the proposed model which has been introduced later. Table (1) shows, the geometric and mass properties of the flexible link which consists of steel flat bar clamped to an electric motor.

Table(1) Geometric & mass properties of the flexible link

parameter	value
Arm length L	0.762 [m]
Cross-section area A	$2.42 * 10^{-4}$ [m ²]
Young's modulus E	$2 * 10^{11}$ [N/m ²]
Specific mass ρ	7836.63 [Kg/ m ³]
Area moment of inertia I _z	$20.655 * 10^{-11}$ [m ⁴]

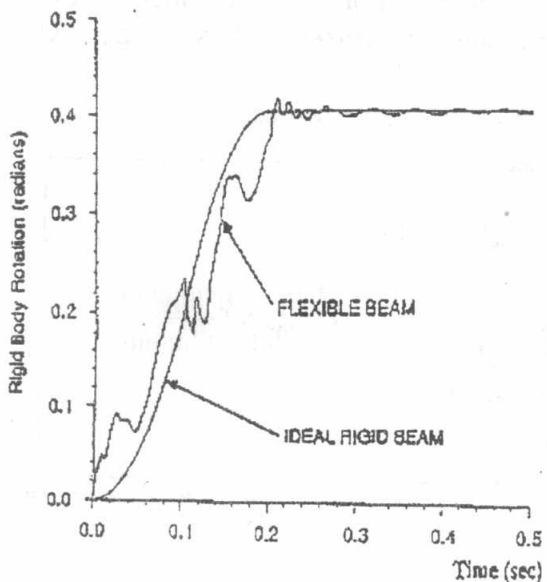


Fig.(3) Time history of the joint angle of the finite element model [1].

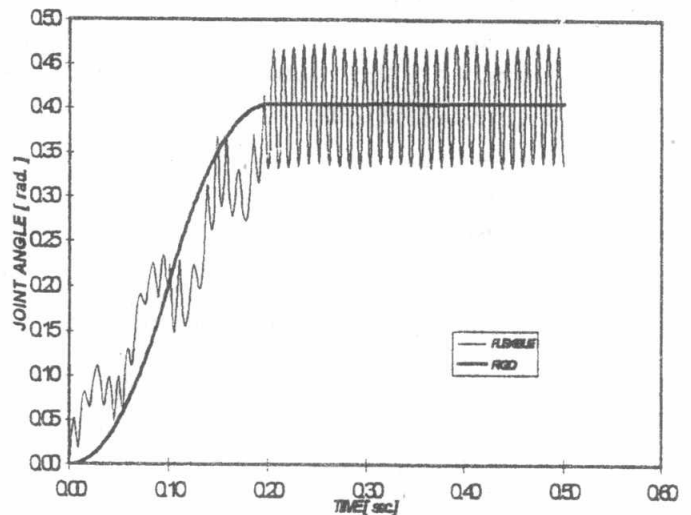


Fig.(4) Time history of the joint angle of the proposed model.

EFFECT OF THE MANIPULATOR FLEXIBILITY.

To evaluate the effect of the manipulator flexibility, the time histories corresponding to the following variables have been calculated:

i-the modification of the joint angle $\Delta\theta$

$$\Delta\theta = \theta_R - \theta_F$$

ii-the manipulator lateral tip displacement v_t .

iii-the slope of the manipulator at the tip point ϕ_t .

These three variables have been calculated in addition of course to the modal coordinates a_1 and a_2 .

Figures(5), and (6) show the time histories of the modal coordinates a_1 and a_2 .

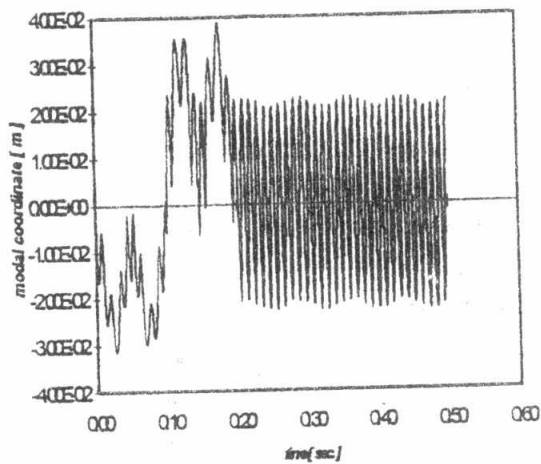


Fig.(5) Time history of the first modal coordinate a_1 .

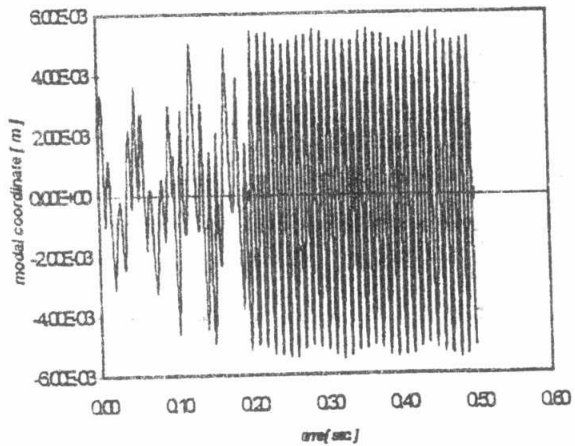


Fig.(6) Time history of the second modal coordinate a_2 .

The analysis of Figs.(5), and (6) shows that, the contribution of the first mode in the dynamic response is greater than the second mode. This corresponds to the general character of the assumed mode method used.

Figures(7), (8), and (9) show the time histories of v_t , ϕ_t , and $\Delta\theta$ respectively.

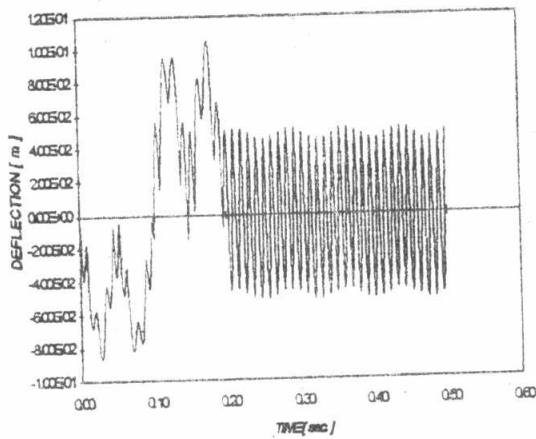


Fig.(7) Time history of the tip point displacement v_t .

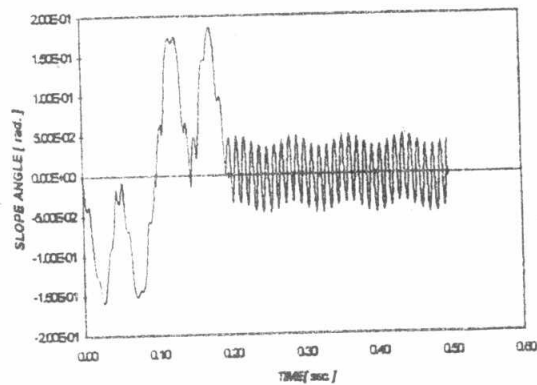


Fig.(8) time history of the slope angle at the tip point.

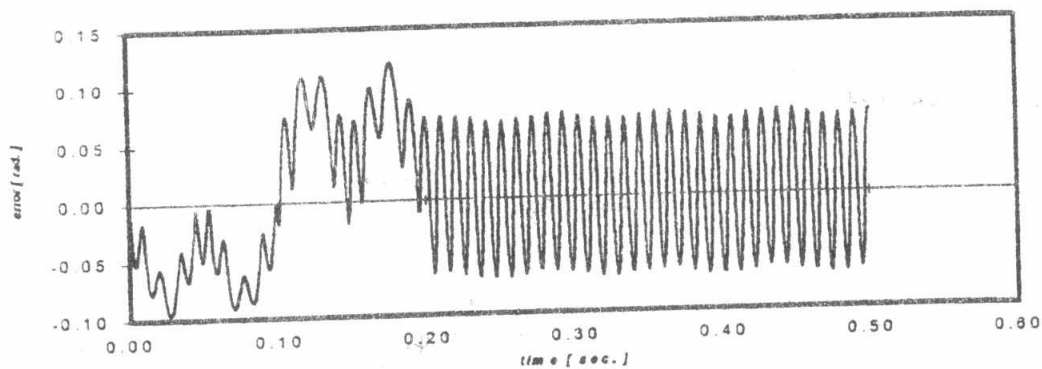


Fig.(9) Time history of the joint angle modification $\Delta\theta$.

The analysis of Figs.(7), (8), (9) shows that, these time histories pass by three distinct time periods $0 \leq t < 0.1$, $0.1 \leq t < 0.2$, and $0.2 \leq t$. The first two time periods represents a transient response. The third one, however, corresponds to a sustained vibration. In the first time period $\Delta\theta$, v_t , and φ_t start at zero values, pass by two dominant maximums and returns to zero again. In the second time period $\Delta\theta$, v_t , and φ_t change their sign and pass by two other maximum values before the sustained vibratory behavior in the third period. This time pattern of $\Delta\theta$, v_t , and φ_t may be correlated to the torque profile used, (see Fig.(2)).

INVESTIGATION OF THE EFFECT OF THE MAIN DESIGN PARAMETERS.

The design goal of a flexible manipulator is achieved when its payload is increased and the vibratory effects are reduced. In this section, therefore, three design parameters will be investigated:

- Effect of damping.
- Effect of payload.
- Effect of open loop control torque profile.

EFFECT OF DAMPING.

The damping introduced here is of viscous type. Rayleigh's Dissipation Function D is introduced as [2],

$$D = \frac{1}{2} \left[\dot{\mathbf{a}} \right]^T [C] \left[\dot{\mathbf{a}} \right]$$

After the normalization with respect to mass, the diagonal matrix $[C]$ is defined as,

$$[C] = \begin{bmatrix} 2\xi_1\omega_1 & 0 \\ 0 & 2\xi_2\omega_2 \end{bmatrix}$$

Lagrange's equations (1) considering Rayleigh's Dissipation Function can be rewritten as,

$$\frac{d}{dt} \left(\frac{\partial T}{\partial \dot{q}_i} \right) - \frac{\partial T}{\partial q_i} + \frac{\partial D}{\partial \dot{q}_i} + \frac{\partial V}{\partial q_i} = Q_i \quad q_i = a_1, a_2.$$

The dynamic response based on the above mentioned equations has been calculated for different values of the modal damping ξ_i . when the manipulator is being subjected to an optimal torque corresponding to rigid rest to rest manoeuvre (see Fig.(2)). The analysis of this study leads to, damping has two main effects on the elastic displacements of the manipulator:

- i- Slit reduction of the maximum values of elastic displacements during the maneuver period $0 \leq t \leq 0.2$ sec.
- ii- Significant reduction and even elimination of the residual vibration after the maneuver period.

The reduction of the maximum values of elastic displacements and the modification of joint angle are best demonstrated on Fig.(10), where, $\Delta\theta_{\max}$, $v_{t\max}$, and $\varphi_{t\max}$ are plotted against ξ .

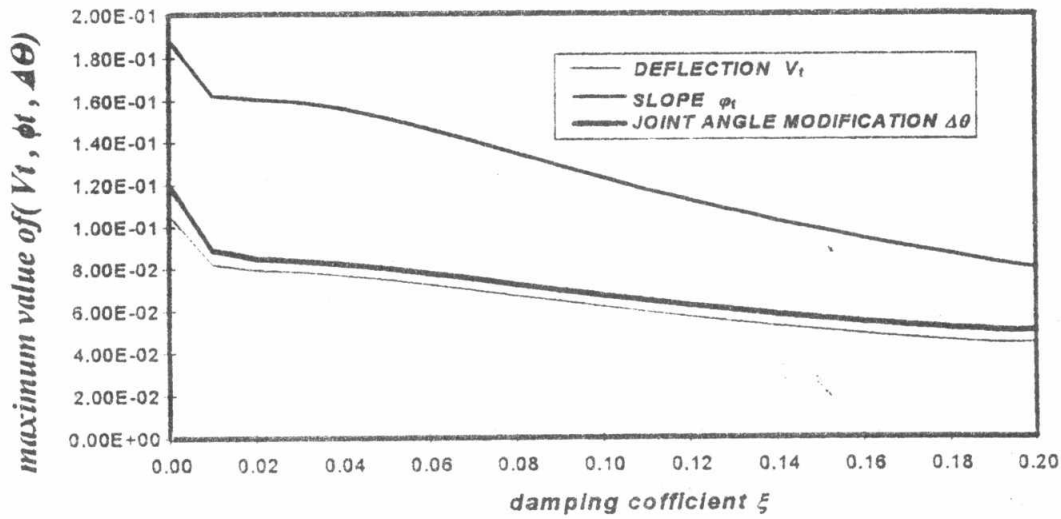


Fig.(10)The variation of the maximum values of elastic displacements with damping ratio ξ .

EFFECT OF PAYLOAD.

The payload is a very important parameter for the design of a flexible manipulator. An important objective of the manipulator mechanical and control design is to increase its payload. It is anticipated, however, that the increase of payload will be accompanied with an increase of the elastic displacement and the residual vibration after performing a manoeuvre. The effect of payload has been investigated by calculating the dynamic response of the manipulator assuming different payload to manipulator mass ratio, (m_p/m). The bang-bang torque profile has been recalculated for each value of (m_p/m) so as to produce the same rigid rest to rest manoeuvre. Fig.(11) show that The variation of the maximum values of elastic displacements with the payload.

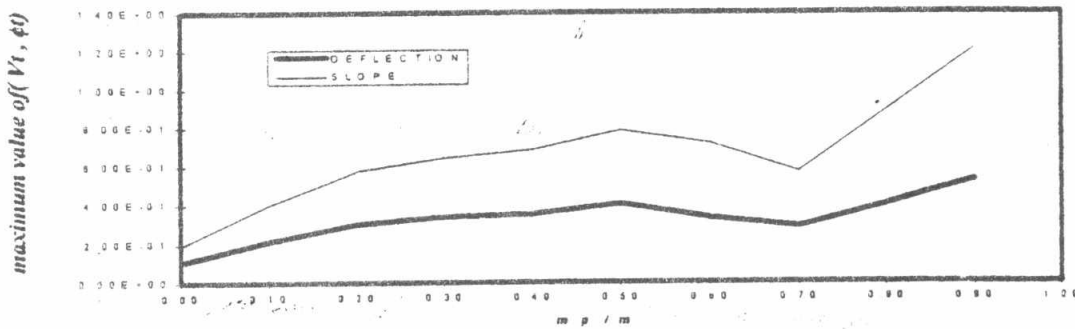


Fig.(11)The variation of the maximum values of elastic displacements with the payload.

The variation of the maximum values of the manipulator elastic displacement represented by $(v_t)_{max}$ and $(\phi_t)_{max}$ increases progressively. The order of magnitude of the tip point displacement for values of $m_p/m > 0.1$ is rather elevated. This situation should be considered in conjunction with the torque profile used. Reasonable values of flexible manipulator displacement may be achieved by limiting the payload (m_p/m to be limited) and the convenient choice of the torque profile corresponding to the required manoeuvre.

EFFECT OF OPEN LOOP CONTROL TORQUE PROFILE.

The torque profile used up till this point is the optimal torque corresponding to rest to rest manoeuvre of a rigid manipulator which is given by Fig.(2). The author has been convinced that there should be certain optimal torque profile which satisfy the useful rigid rest to rest manoeuvre and at the same time reduces the transient and steady state elastic motion (vibration). It is for that reason that two extra torque profiles have been investigated, a triangular torque profile Fig.(12) and a trapezoidal torque profile Fig.(14). The magnitude of these torques are calculated such that the rigid rest to rest manoeuvre is kept the same. The dynamic response of the manipulator under the triangular torque profile is shown in Figs(13). The dynamic response of the manipulator under the trapezoidal torque profile is, however, shown in Figs.(15).

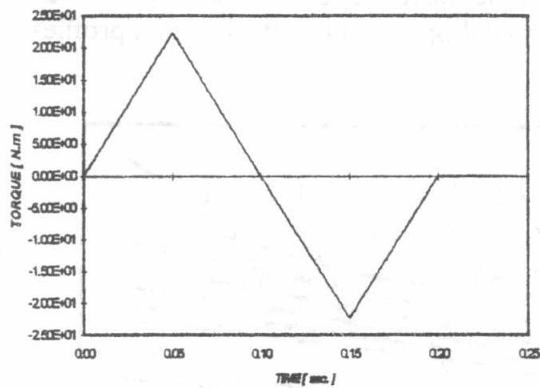


Fig.(12) triangular torque profile .

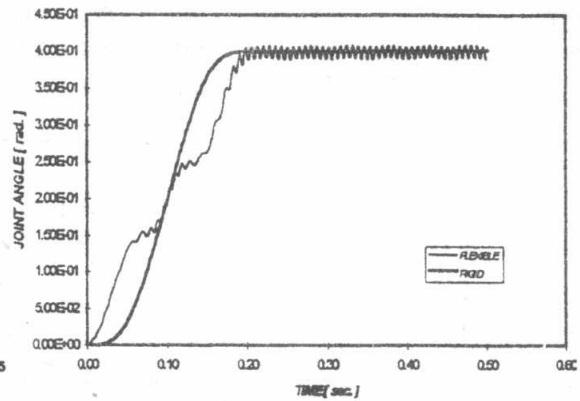


Fig.(13) The joint angle θ for flexible and rigid case corresponding to the triangular torque profile .

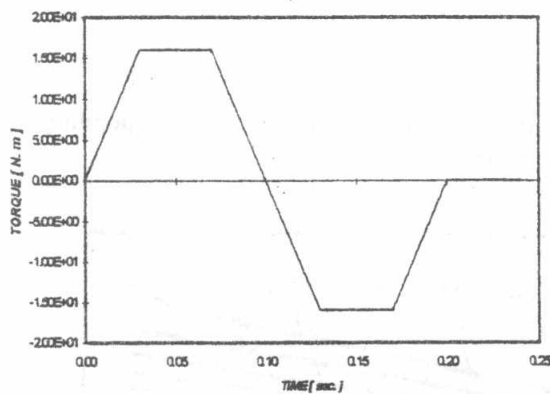


Fig.(14) Trapezoidal torque profile .

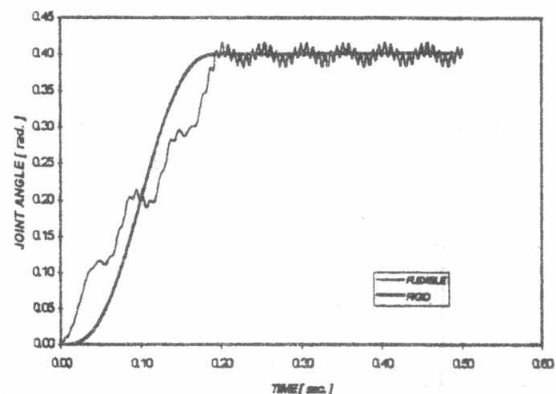


Fig.(15) The joint angle θ for flexible and rigid case corresponding to the trapezoidal torque profile .

The comparison between Fig.(4), Fig.(13), and Fig.(15), shows that the order of magnitude of the maximum manipulator deflection during the transient manoeuvre period is practically the same for the three torque profiles investigated. the triangular torque profile, however, is associated with the sustained vibration having minimum magnitude.

COLLECTIVE PARAMETRIC ANALYSIS.

The effect of modal damping, payload, and open loop control torque profile on the dynamic response of the manipulator have been investigated individually. The analysis of time histories corresponding to the manipulator tip point elastic displacement v_t and elastic rotation ϕ_t for each case shows that they follow practically the same pattern. i.e. v_t and ϕ_t pass by extremum values for $0 < t \leq 0.1$ sec. then they change their sign and pass by other extremum values for $0 \leq t \leq 0.2$. For $0.2 < t$, sustained vibration is obtained. To demonstrate the effect of the design parameters collectively the magnitude of the maximum values over the time histories of v_t and ϕ_t have been presented for bang-bang, triangular, and trapezoidal open loop control torque profiles respectively on Figs.(16), (17), and (18).

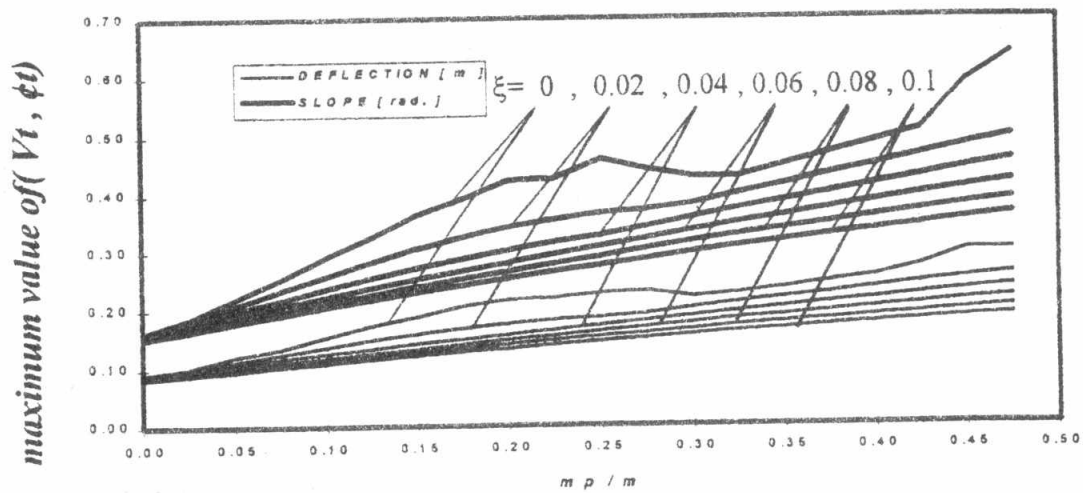


Fig.(16)Effect of payload and damping on the tip point deflection and slope angle corresponding to the triangular torque profile .

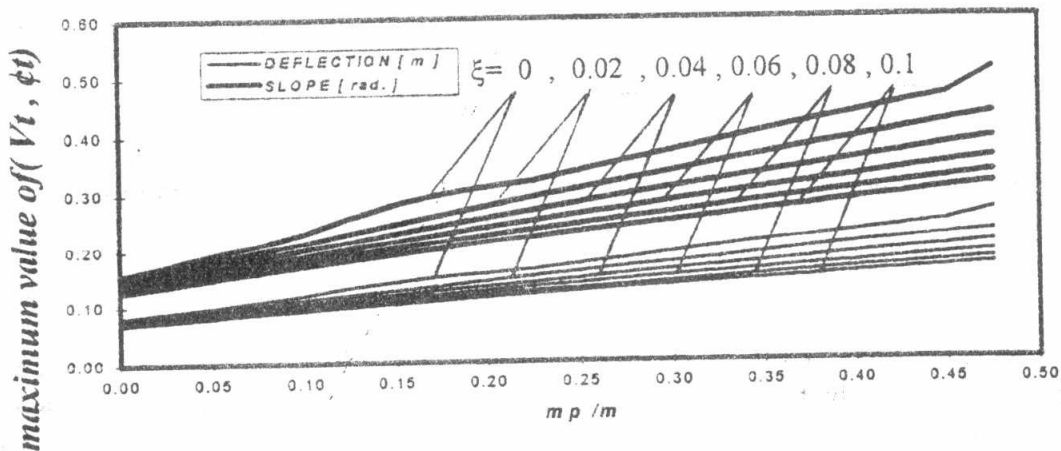


Fig.(17) Effect of payload and damping on the tip point deflection and slope angle corresponding to the trapezoidal torque profile .

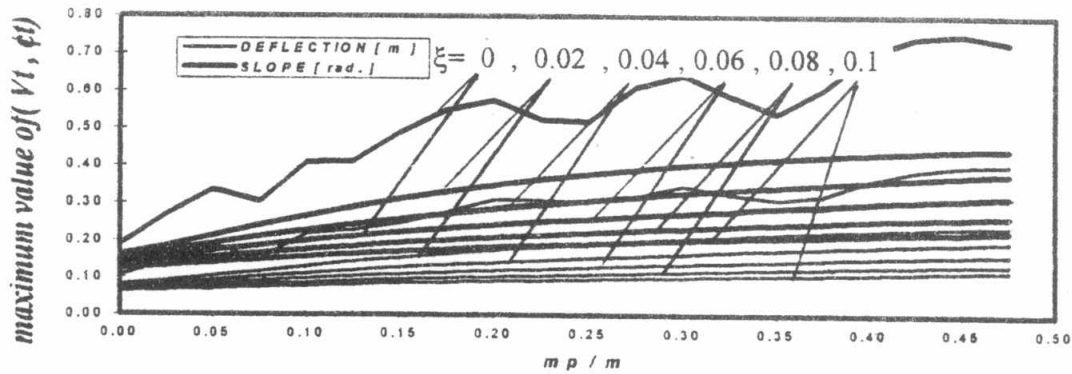


Fig.(18)Effect of payload and damping on the tip point deflection and slope angle corresponding to the bang-bang torque profile .

The analysis of Figs.(16), (17), and (18) shows that:

- The payload has a very important effect on the tip point elastic deflection and rotation.
- The increase of damping reduces the tip point elastic deflection and rotation.

The triangular open loop control torque profile creates the lowest tip point elastic deflection and rotation compared with the bang-bang and the trapezoidal open loop control torque profile.

CONCLUSION.

The Lagrangian mechanics and the assumed mode method have been used to drive a proposed dynamic model of a single link flexible manipulator having a revolute joint. The model may be used in general to investigate the motion of the manipulator in the vertical plane. The validity of the proposed model has been verified through the comparison between the dynamic response of the manipulator based on the proposed model and that based on a Finite Element model [1]. Quite satisfactory agreement has been recognized between the dynamic response based on both models. The proposed model has been used to investigate the effect of three main design parameters, the payload, the damping, and the open loop control torque profile. The results of investigation show that as long as the rest to rest rotational manouevre is considered, the payload has a dominant effect on the elastic deflection of the manipulator. The increase of damping reduces the elastic deflection and the residual vibration. The increase of damping is, however, limited by the availability of an energy absorption material layer to be integrated with the link structure. The minimum values of elastic manipulator deflection have been achieved using a triangular shaped open loop control torque profile.

REFERENCES.

- [1]Daniel, W. W., "Finite Element Based Dynamic Modeling of Flexible Open-Loop Manipulators with Experimental Results." Ph. D. Thesis. University of Wisconsin-Madison,1990.
- [2]Rao, S. S., "Mechanical Vibration," Addison, Wesley Company, 1986.
- [3] Petroka, R. P., and Chang, L. W., "Experimental Validation of a Dynamic Model (Equivalent Rigid Link System) on a Single-Link Flexible Manipulator," ASME Journal of Dynamic Systems, Measurement and Control, Vol. 111, Dec. 1989, pp. 667-672.
- [4] Chang, L. W., and Gannon, K. P., "A Dynamic Model On a Single Link Flexible Manipulator," ASME Journal of Vibration and acoustics, Vol. 112, January 1990, pp. 138-143.